Human embryonic stem cell microenvironment suppresses the tumorigenic phenotype of aggressive cancer cells

Lynne-Marie Postovit*, Naira V. Margaryan, Elisabeth A. Seftor, Dawn A. Kirschmann, Alina Lipavsky, William W. Wheaton, Daniel E. Abbott, Richard E. B. Seftor, and Mary J. C. Hendrix†

Program in Cancer Biology and Epigenomics, Children's Memorial Research Center, Feinberg School of Medicine, Northwestern University, Chicago, IL 60614

Communicated by Richard D. Klausner, The Column Group, Seattle, WA, January 21, 2008 (received for review July 1, 2007)

Embryonic stem cells sustain a microenvironment that facilitates a balance of self-renewal and differentiation. Aggressive cancer cells, expressing a multipotent, embryonic cell-like phenotype, engage in a dynamic reciprocity with a microenvironment that promotes plasticity and tumorigenicity. However, the cancer-associated milieu lacks the appropriate regulatory mechanisms to maintain a normal cellular phenotype. Previous work from our laboratory reported that aggressive melanoma and breast carcinoma express the embryonic morphogen Nodal, which is essential for human embryonic stem cell (hESC) pluripotency. Based on the aberrant expression of this embryonic plasticity gene by tumor cells, this current study tested whether these cells could respond to regulatory cues controlling the Nodal signaling pathway, which might be sequestered within the microenvironment of hESCs, resulting in the suppression of the tumorigenic phenotype. Specifically, we discovered that metastatic tumor cells do not express the inhibitor to Nodal, Lefty, allowing them to overexpress this embryonic morphogen in an unregulated manner. However, exposure of the tumor cells to a hESC microenvironment (containing Lefty) leads to a dramatic down-regulation in their Nodal expression concomitant with a reduction in clonogenicity and tumorigenesis accompanied by an increase in apoptosis. Furthermore, this ability to suppress the tumorigenic phenotype is directly associated with the secretion of Lefty, exclusive to hESCs, because it is not detected in other stem cell types, normal cell types, or trophoblasts. The tumor-suppressive effects of the hESC microenvironment, by neutralizing the expression of Nodal in aggressive tumor cells, provide previously unexplored therapeutic modalities for cancer treatment.

Lefty | Nodal | melanoma | breast carcinoma

Metastatic cancer cells resemble stem cells in their ability to self-renew and to derive a diverse progeny. Moreover, the phenotype of stem cells and cancer cells is profoundly influenced by the microenvironment. During embryogenesis, precursor cells are specified to particular fates through the delivery of signaling molecules, and malignant cells similarly release and receive cues that promote tumor growth and metastasis. There also is a convergence between cancer cells and stem cells in the molecular messengers they implement to regulate self-renewal and cell fate. These stem-cell-associated factors include members of the Notch, Wingless, and transforming growth factor β (TGF-β) superfamilies (1–7). Particularly noteworthy are recent findings involving Nodal, an embryonic morphogen belonging to the TGF-β superfamily (4). Overexpression of Nodal prevents hESC differentiation, and inhibiting Nodal signaling in metastatic melanoma cells results in decreased colony formation in soft agar concomitant with a marked abrogation of tumor formation in an orthotopic mouse model (4, 8). Furthermore, we have shown that the Nodal secreted by metastatic melanoma cells is functional, as demonstrated by the induction of Nodal-responsive genes and ectopic tissues in embryonic zebrafish transplanted with these tumor cells (4).

The multipotent phenotype of metastatic cancer cells permits them to respond to cues normally restricted to developmental processes (1). Hence, we hypothesized that embryonic microenvironments, which are inherently permissive to normal stem cell differentiation, may be used to reprogram (i.e., redifferentiate) cancer cells toward a benign phenotype. Indeed, embryonic microenvironments have been shown to inhibit the tumorigenicity of a variety of cancer cell lines (1, 9–11). For example, the mouse embryonic microenvironment can reprogram teratocarcinoma cells to a nontumorigenic phenotype capable of differentiating into normal tissues (11), and extracts derived from zebrafish embryos can inhibit proliferation and induce apoptosis in a number of cancer cell types. Moreover, we have demonstrated that exposure of metastatic melanoma cells to an embryonic zebrafish microenvironment, before gastrulation, results in their reprogramming toward a nontumorigenic phenotype (12, 13) and that metastatic melanoma cells transplanted into developing chick embryos are capable of following neural crest migration pathways, resulting in a loss of tumorigenicity and the acquisition of a neural crest-like phenotype (10).

To elucidate the mechanisms by which embryonic microenvironments reprogram cancer cells to a more differentiated, less aggressive phenotype, so that humanized therapeutic modalities may be discovered, we developed an *in vitro* 3D model to investigate the capacity of hESC-derived factors to epigenetically influence metastatic cancer cells (1, 14). Using this approach, we previously determined that exposure of melanoma cells to a hESC microenvironment results in the reexpression of melanocyte-specific markers (illustrative of redifferentiation) and a reduction in invasive potential (1, 14). However, the molecular underpinnings of the reprogramming potential of the hESC microenvironment remained elusive. In the current study, we have discovered that hESC microenvironments suppress the tumorigenic phenotype of human metastatic melanoma and breast carcinoma cells and that this effect is exclusive to hESCs and not other stem cell types derived from amniotic fluid, cord blood, or adult bone marrow. Mechanistically, the hESC microenvironment specifically neutralizes the aberrant expression of Nodal in metastatic melanoma and breast carcinoma

Author contributions: N.V.M. and E.A.S. contributed equally to this work. L.-M.P., E.A.S., R.E.B.S., and M.J.C.H. designed research; L.-M.P., N.V.M., E.A.S., D.A.K., A.L., W.W.W., D.E.A., and R.E.B.S. performed research; L.-M.P., E.A.S., and R.E.B.S. contributed new reagents/analytic tools; L.-M.P., N.V.M., E.A.S., D.A.K., R.E.B.S., and M.J.C.H. analyzed data; and L.-M.P., R.E.B.S., and M.J.C.H. wrote the paper.

The authors declare no conflict of interest.

*Present address: Department of Anatomy and Cell Biology, Schulich School of Medicine and Dentistry, University of Western Ontario, Medical Sciences Building, Room 438, London, ON, Canada N6A 5C1.

†To whom correspondence should be addressed at: Children's Memorial Research Center, Feinberg School of Medicine, Northwestern University, 2300 Children's Plaza, Box 222, Chicago, IL 60614-3394. E-mail: mjchendrix@childrensmemorial.org.

This article contains supporting information online at www.pnas.org/cgi/content/full/0800467105/DC1.

cells, reprogramming them to a less aggressive phenotype exemplified by diminished clonogenicity and tumorigenicity (with apoptosis). Moreover, we uncovered hESC-secreted Lefty (an inhibitor of Nodal signaling) as an important mediator of these phenomena. The microenvironment of hESCs provides a previously unexplored therapeutic entity for the regulation of aberrantly expressed embryonic factor(s) in aggressive tumor cells.

Results

Characterization of Nodal Signaling Pathway Members in Human Normal Cells, Metastatic Cancer Cells, Human Embryonic Stem Cells (hESC), and Other Stem Cell Types. To better characterize the role of Nodal in the maintenance of pluripotency and tumorigenicity, we examined the expression of key components of the Nodal signaling pathway in human normal, neoplastic and stem cell types. Western blot analyses revealed that in a manner similar to hESCs (MEL-2, H1, and H9), metastatic melanoma (C8161) and breast carcinoma (MDA-MB-231) cells express Nodal protein at ≈48 kDa (Fig. 1*A*). This is in contrast to corresponding normal cell types [melanocytes, myoepithelial cells (Hs 578 Bst), and primary human mammary epithelial cells (HMEpC)], in which Nodal was not detected. Using RT-PCR, we determined that Nodal is expressed in additional melanoma (WM278), and breast carcinoma (T47D, MDA-MB-468, MDA-MB-330, and ZR75–30) cell lines [supporting information (SI) Fig. 5*A*]. Nodal propagates its signal by binding to a receptor complex comprised of Cripto and a heterodimer of type I (ALK 4/7) and type II (ActRIIB) activin-like kinase receptors. Genetic studies in zebrafish and mice have determined that Cripto directly associates with ALK 4 and Nodal and that these associations facilitate the ability of Nodal to propagate its signal (15, 16). Using Western blot analysis and immunofluorescence microscopy, we determined that hESCs uniformly express high levels of Cripto at ≈35 kDa; however, only a low level of Cripto was heterogeneously expressed in C8161 and MDA-MB-231 cells (Fig. 1 *A* and *B*). Moreover, only one additional melanoma line (WM278) and two additional breast carcinoma lines (T47D and ZR75–30) examined in this study expressed detectable levels of Cripto transcript (SI Fig. 5*A*).

The Lefty proteins (Lefty-A and Lefty-B), divergent members of the TGF-β superfamily, spatially and temporally antagonize Nodal in embryological systems (17). Moreover, the Lefty genes are downstream targets of Nodal signaling, thereby providing a powerful negative-feedback loop for this pathway (17). By using Western blot analysis we determined that, in accordance with previously published accounts of Lefty protein processing patterns, hESCs express Lefty protein at ≈42, 34 and 28 kDa (17, 18). In contrast, Lefty is not expressed by metastatic breast carcinoma and melanoma cells or by corresponding normal somatic cell types (Fig. 1*A* and SI Fig. 5*A*). To visualize the localization of Lefty and Nodal in hESC colonies and their microenvironment, we performed immunofluorescence localization with confocal microscopy. Using this method, we determined that Lefty protein localizes to the areas where hESCs contact the underlying Matrigel matrix, and that hESC-derived Lefty permeates into this microenvironment (Fig. 1*C*). This is in contrast to Nodal protein, which localizes to the surface of hESC colonies, and is secreted into the media. These results were confirmed with Western blot analyses, which demonstrated that Lefty protein can be detected in Matrigel conditioned by H9 hESCs (H9 CMTX; Fig. 1*C*). Furthermore, neither Nodal nor Lefty is found in unconditioned control Matrigel alone (data not shown).

We next sought to elucidate the expression of Nodal, Lefty, and Cripto in other human stem cell types and in first trimester human cytotrophoblast cells (HTR-8/SVneo). Western blot analyses revealed that umbilical-cord-derived mesenchymal stem cells (MSC; SC00125) and adult MSCs do not express Nodal and Cripto, and that although amniotic-fluid-derived stem cells (GM00473, GM00957A) and cytotrophoblast cells express Cripto, only the latter expresses appreciable levels of Nodal (SI Fig. 5*B*). Of note, in contrast to hESCs, none of the other stem cell lines examined expressed an appreciable level of Lefty protein (SI Fig. 5*B*). To

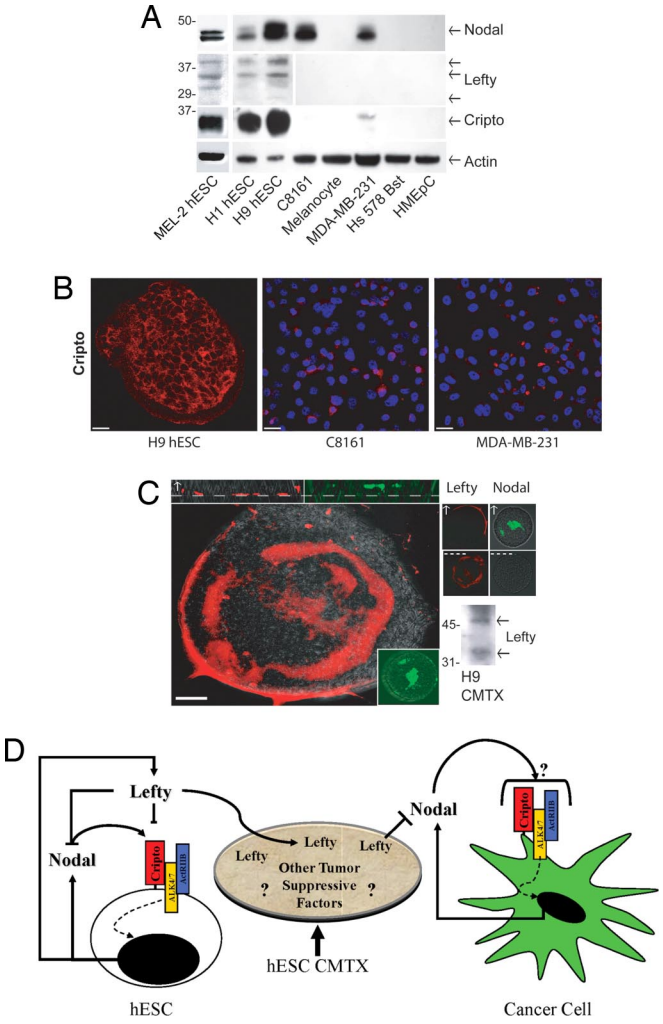

Fig. 1. Characterization of Nodal signaling pathway members. (*A*) Western blot analyses of Nodal, Lefty, and Cripto in: MEL-2, H1, and H9 hESCs; C8161, human metastatic melanoma cells; normal human melanocytes; MDA-MB-231, human metastatic breast carcinoma cells; Hs 578 Bst normal human myoepithelial cells; and HMEpC normal human mammary epithelial cells. Actin is used as a loading control. (*B*) Immunofluorescence localization of Cripto (red) in ≈100% of H9 hESCs and in small subpopulations of C8161 and MDA-MB-231 cells. Cell nuclei are counterstained blue with DAPI. (Scale bar: 10 μm.) (*C*) Immunofluorescence localization of Lefty (red) and Nodal (green) in H9 hESCs cultured on Matrigel and Western blot analysis of Lefty protein in matrix conditioned by hESCs (H9 CMTX). (*Top*) Reconstructed confocal images depicting the cross-section of a hESC colony with its underlying matrix. Dashed line designates the cell-matrix interface, and the arrow points to the upper surface of the hESC colony. Corresponding images on the right illustrate Lefty and Nodal at the cell surface (arrow) and the cell-matrix interface (dashed line). The large image is a 3D confocal projection of hESC colonies stained with Lefty (distributed in the matrix microenvironment) and Nodal (*Inset*), associated with the hESCs. (Scale bar: 25 μm.) (*D*) Putative signaling model outlining how hESCs may reprogram metastatic cancer cells by inhibiting Nodal signaling. Nodal initiates a signaling cascade by binding to a receptor complex consisting of Cripto, type I (ALK 4/7), and type II (ActRIIB) activin-like kinase receptors and is regulated via a positive feedback loop. hESCs also secrete Nodal inhibitors, including Lefty, which is up-regulated in response to Nodal but antagonizes the Nodal signaling pathway by interacting with Nodal and/or Cripto. Like hESCs, cancer cells also express Nodal, whereas unlike hESCs they do not express Lefty. HESC-derived Lefty, found in hESC conditioned matrices (CMTX), may inhibit Nodal signaling in cancer cells and promote their reprogramming toward a less malignant phenotype. Other tumor suppressive factors also may be deposited by the hESCs.

confirm the apparent exclusivity of Lefty expression to hESCs, we performed real-time RT-PCR. Using this method, we determined that relative to hESCs, metastatic cancer cells, normal somatic cells and trophoblast cells do not express appreciable levels of *Lefty* mRNA (SI Fig. 5*C*). Moreover, the other stem cell types used in this study expressed a comparably insignificant level of *Lefty* (SI Fig. 5*C*). We previously demonstrated that Nodal expression is positively correlated with melanoma progression, such that Nodal protein is not expressed in normal melanocytes or radial growth phase melanomas, but is present in vertical growth phase and metastatic lesions (4). The current study characterized Nodal localization (previously unexplored) in breast tissues: Using immunohistochemical analysis of a human breast tissue microarray (TMA) we observed that Nodal protein is absent in normal breast tissue, and that its expression is positively correlated with breast cancer progression ($P < 0.05$; SI Fig. 5*D* and SI Table 1). Given the significant observation that like hESCs, cancer cells express Nodal, although unlike hESCs, they do not express Lefty, we hypothesized that hESC-derived Lefty and possibly other tumor-suppressive factors found in hESC-conditioned matrices (CMTX), may inhibit Nodal signaling in cancer cells (Fig. 1*D*). We further proposed that by neutralizing Nodal in cancer cells, hESC microenvironments will reprogram these tumor cell types toward a less tumorigenic phenotype.

Exposure of Cancer Cells to hESC-Derived Factors, Particularly Lefty, Results in Decreased Nodal Expression Concomitant with Reduced Clonogenicity. To examine the effect of hESC-derived Lefty on tumor cell phenotype, we used Dynabeads covalently coupled to anti-Lefty antibody to isolate Lefty from hESCs cultured on a feeder-free Matrigel matrix. The specificity and utility of the anti-Lefty antibody used to recover Lefty protein was confirmed by Western blot analysis and corresponding Coomassie stained SDS/PAGE of known rLefty-A and -B standards whose sequences were subsequently confirmed by liquid chromatography/mass spectrometry (LC/MS; SI Fig. 6*A*). Purified hESC-derived Lefty was seeded into Matrigel and the effects of the "Lefty-containing" matrix on cancer cell phenotype were determined. Western blot analysis revealed that hESC-derived Lefty significantly diminished Nodal protein expression in C8161 and MDA-MB-231 cells (Fig. 2*A*).

To further substantiate the specificity of these results, the cancer cells were also exposed to Matrigel conditioned by hESCs in which Lefty protein expression was knocked down with FITC-tagged Morpholinos specific for Lefty-A and Lefty-B (MO^{LEFTY}). [The fluorescently tagged Morpholinos could be detected microscopically in >75% of the hESC colonies treated (SI Fig. 6*B Upper*), and Western blot analysis confirmed the efficient knock down of Lefty protein in hESCs for up to 3 days (SI Fig. 6*B Lower*)]. The expression of *Oct-3/4* and *Nanog*, representative of pluripotency, was not affected during this time, and morphology of the hESC colonies was not altered (SI Fig. 6*C*). Thus, although MO^{LEFTY} knocked down Lefty protein in the hESCs, it did not induce stem cell differentiation during this window of observation. Western blot analysis revealed that C8161 and MDA-MB-231 cells up-regulate Nodal protein expression in response to this "H9 Lefty-deficient" hESC matrix (Fig. 2*B*). C8161 and MDA-MB-231 cells treated with rNodal (100 ng/ml) similarly experienced an up-regulation of *Nodal* mRNA expression (SI Fig. 6*D*), and hESCs treated with MO^{LEFTY} up-regulated Nodal protein expression (Fig. 2*B*). These findings are in accordance with the positive feed-back loop that characterizes the Nodal signaling pathway. In contrast to rNodal, which has biological activity, previous studies have reported that recombinant Lefty protein (rLefty) is unable to inhibit Nodal signaling (17). We confirmed these results and extended them to discover that rLefty-B can inhibit Nodal protein in C8161 cells, but at a non-physiological dose (1,000 ng/ml) (SI Fig. 6*E*). In an effort to understand the disparate results between hESC-derived Lefty and rLefty on Nodal signaling, we analyzed glycoprotein content in

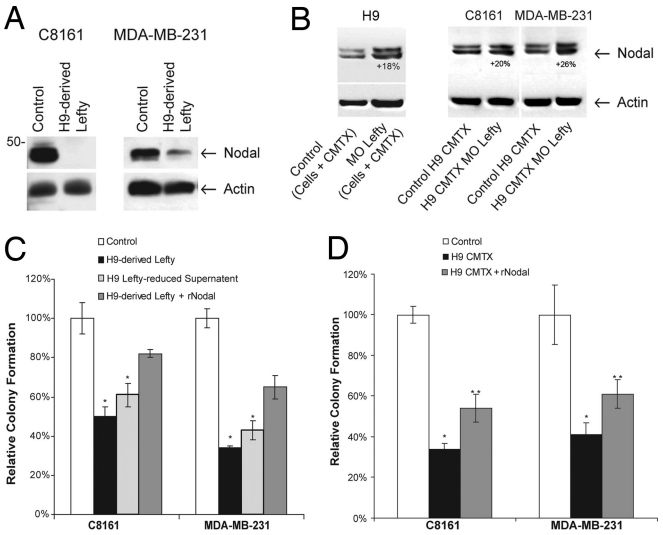

Fig. 2. Exposure of cancer cells to hESC-derived Lefty decreases Nodal expression concomitant with reduced anchorage-independent growth. (*A*) Western blot analysis of Nodal protein in C8161 and MDA-MB-231 cells exposed for 3 days to either unconditioned control Matrigel or to Matrigel seeded with Lefty protein purified from hESCs (H9-derived Lefty). MDA-MB-231 cells were allowed to recover on fresh Matrigel for 2 days before analysis. Actin is used as a loading control. (*B*) Western blot analyses of Nodal protein in H9 hESCs treated with either $MO^{Control}$ or MO^{Lefty} and Nodal protein levels in C8161 and MDA-MB-231 cells cultured for 3 days on Matrigel conditioned by hESCs treated with either $MO^{Control}$ or MO^{Lefty}. Numbers represent percentage change between $MO^{Control}$ and MO^{Lefty} group determined by using densitometric analysis. (*C*) Relative colony formation of C8161 and MDA-MB-231 cells cultured on soft agar for 14 days after 3 days of exposure to control Matrigel, Matrigel seeded with Lefty purified from hESCs (H9-derived Lefty), or Matrigel seeded with Lefty-reduced hESC supernatant. Assay was conducted in the presence or absence of rNodal (100 ng/ml). Bars represent mean normalized colony formation ± SD, and values indicated by an asterisk (*) are significantly different from the colony-forming ability of control cells ($n = 6$, $P < 0.05$). (*D*) Relative colony formation of C8161 and MDA-MB-231 cells cultured on soft agar for 14 days after 3 days of exposure to control Matrigel or to H9 CMTX. Assays were conducted in the presence or absence of rNodal (100 ng/ml). Bars represent mean normalized colony formation ± SD, and values indicated by an asterisk (*) are significantly different from the colony-forming ability of control cells whereas values indicted by a double asterisk (**) are significantly different from the colony-forming ability of control cells and H9 CMTX treated cells ($n = 12$, $P < 0.05$).

rLefty-B, rLefty-A and a lysate from the H9 hESCs plus their CMTX. We determined that in an apparent contrast to the rLefty proteins, H9-derived Lefty is glycosylated (SI Fig. 6*F*).

As a functional correlate, we determined that exposure of C8161 and MDA-MB-231 cells to H9 Lefty-derived matrix significantly reduces anchorage-independent growth, and that this inhibition of *in vitro* clonogenicity can be rescued by the inclusion of recombinant Nodal (rNodal; 100 ng/ml) (Fig. 2*C*). Furthermore, exposure of C8161 and MDA-MB-231 cells to H9 CMTX reduced their ability to undergo anchorage-independent growth but this inhibition of *in vitro* clonogenicity was only partially rescued by the inclusion of rNodal (100 ng/ml) (Fig. 2*D*). In addition, hESC supernatant inhibited anchorage-independent growth, even when Lefty was decreased via the aforementioned Dynabead isolation, although not to the same level as purified Lefty. Collectively, these findings suggest that hESC-derived Lefty has important anti-tumorigenic potential, but that it is not the only tumor suppressive factor within this unique embryonic microenvironment.

We next determined the effects of H9 CMTX on Nodal expression in C8161 and MDA-MB-231 cells. Real-time RT-PCR showed that exposure to H9 CMTX down-regulates *Nodal* mRNA expression in both C8161 and MDA-MB-231 cells, and that this effect is reversible over time (Fig. 3*A*). Exposure to H9 CMTX similarly

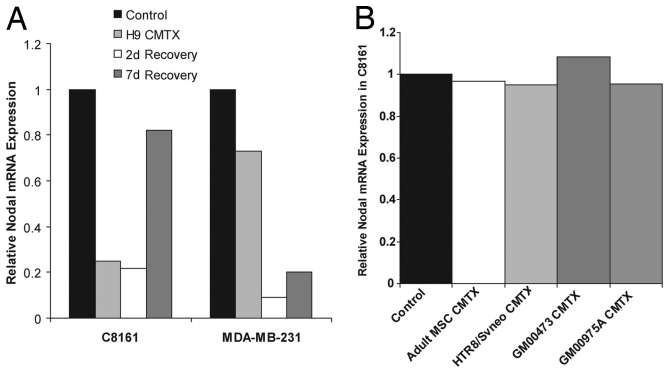

Fig. 3. The microenvironment of hESCs, containing Lefty, down-regulates Nodal expression in melanoma and breast carcinoma cells. (*A*) Real-time RT-PCR analysis of *Nodal* mRNA in C8161 and MDA-MB-231 cells exposed for 3 days to either control (unconditioned) Matrigel or to Matrigel conditioned by hESCs (H9 CMTX). Some cancer cells exposed to H9 CMTX subsequently were recovered on control Matrigel for 2 or 7 days before analysis. Gene levels were normalized by using 18S, and bars represent mean gene expression normalized to Matrigel. (*B*) Real-time RT-PCR analysis of *Nodal* mRNA in C8161 cells exposed for 3 days to either control Matrigel or to Matrigel conditioned by adult MSCs, amniotic-fluid-derived stem cells (GM00473/GM00957A CMTX) or trophoblast cells (HTR-8/SVneo CMTX). Gene levels were normalized by using 18S, and bars represent mean gene expression normalized to H9 Matrigel values.

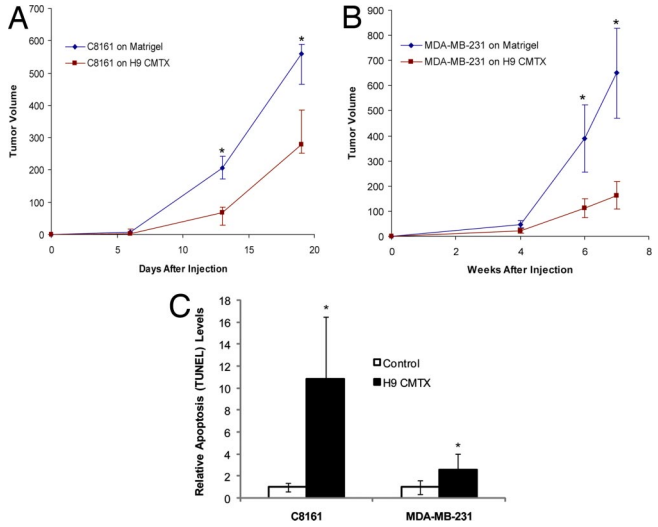

Fig. 4. The microenvironment of hESCs inhibits tumorigenicity. *In vivo* tumor formation in a mouse injected with C8161 cells preexposed for 3 days to either a control matrix (Matrigel) or a matrix conditioned by hESCs (H9 CMTX) ($n = 21$) (*A*) or MDA-MB-231 cells preexposed for 3 days to either a control matrix (Matrigel) or a matrix conditioned by hESCs (H9 CMTX) ($n = 10$) (*B*). Values represent the median tumor volume (mm^3) ± interquartile range (*A*) or the mean tumor volume (mm^3) ± SE (*B*). Tumor volumes were significantly different at the time points indicated by an asterisk (*, $P < 0.05$). (*C*) Tumor cell apoptosis in C8161 and MDA-MB-231-derived tumors determined by TUNEL staining. Before injection into a mouse, C8161 and MDA-MB-231 cells were cultured for 3 days on control or hESC-conditioned (H9 CMTX) matrices. Bars represent mean normalized values ± SD, and values indicated by an asterisk (*) are significantly different from control values ($P < 0.05$).

decreases Nodal protein expression in these cells (SI Fig. 7*A*). Exposure of C8161 cells to matrices conditioned by adult bone-marrow-derived stem cells (MSC), amniotic-fluid-derived stem cells (GM00473, GM00957A), or cytotrophoblast cells (HTR-8/SVneo) did not inhibit Nodal mRNA or protein expression (Fig. 3*B* and SI Fig. 7*B*), thus illuminating the exclusivity of the epigenetic influence of the hESC microenvironment.

The Microenvironment of hESCs Inhibits Melanoma and Breast Carcinoma Tumorigenicity. We implemented orthotopic mouse models to examine the effects of the hESC microenvironment on the *in vivo* tumorigenicity of melanoma and breast carcinoma cells. Exposure of C8161 and MDA-MB-231 cells to H9 CMTX resulted in a significant reduction in tumorigenicity compared with cells exposed to unconditioned Matrigel (Fig. 4 *A* and *B*). To establish a mechanism for the reduction in tumorigenicity, we examined the effects of this treatment on *in vivo* tumor cell proliferation and apoptosis. Using immunohistochemical staining for Ki67 as a measure of proliferation, and terminal deoxynucleotidyl transferase biotin-dUTP nick-end labeling (TUNEL) as a measure of apoptosis, we found that exposure to hESC CMTX decreased proliferation and increased apoptosis in C8161 and MDA-MB-231 cells (Fig. 4*C* and SI Fig. 8). These *in vivo* data confirm the tumor suppressive effects of the hESC microenvironment on aggressive melanoma and breast cancer cells and implicate the potential involvement of apoptotic pathways.

Discussion

Studies dating back to the 1970s and continuing to present day have documented the ability of embryonic microenvironments to reprogram cancer cells toward a benign phenotype (1, 19); however, the mechanisms underlying this phenomenon have remained largely illusive. This study applied an *in vitro* hESC model to specifically demonstrate the anti-tumorigenic properties of the human embryonic microenvironment, and the possible underlying mechanisms. Of significance, our results indicate that: (*i*) The tumor suppressive effects of the microenvironment are exclusive to hESCs, but not other stem cell types; (*ii*) the hESC microenvironment neutralizes the expression of the embryonic morphogen Nodal in metastatic melanoma and breast carcinoma cells, reprogramming them to a less aggressive phenotype exemplified by diminished clonogenicity and tumorigenicity (with increased apoptosis); and (*iii*) Lefty, an inhibitor of the Nodal signaling pathway, is secreted into the hESC microenvironment and is an important mediator of these tumor-suppressive effects. These findings illuminate an embryological signaling pathway that is aberrantly reexpressed in metastatic melanoma (neural crest derived) and breast carcinoma cells (epithelial origin) that could be targeted for the reprogramming of aggressive tumor cells with unique embryonic regulator(s).

Nodal is required to preserve the pluripotency of hESCs and our recent work revealed that Nodal signaling maintains the dedifferentiated multipotent phenotype of highly metastatic C8161 melanoma cells (4, 20, 21). The present study showed that this protein is restricted to aggressive cancer cells, embryonic stem cells, and trophoblasts, and that it is not associated with normal differentiated cell types or with more specified MSCs. Hence, Nodal expression was restricted to embryonic and cancer cell types. Of note, the Nodal gene has been sequenced in the hESCs and melanoma cells used in this study, and no differences or point mutations have been detected (M. Bento Soares, personal communication). This study further demonstrated that Cripto, a prominent mediator of the Nodal signaling pathway in embryological systems, also is restricted to multipotent cancer and stem cell fates. Previous studies, from other laboratories, determined that like Nodal, Cripto is expressed in cancer, specifically testicular, colon and breast cancer cells, but is rarely detected in normal adult tissues (22–24). Furthermore, Cripto is a stem cell marker for pluripotent hESCs and has been associated with dedifferentiation, vascularization and invasion in breast carcinoma cells (23, 25, 26). These functions mirror those of Nodal in melanoma, inferring a convergence of their tumor-promoting functions. Relative to hESCs, Cripto was very weakly and heterogeneously expressed in the metastatic melanoma and breast carcinoma cells used in this study. This finding is intriguing, and raises the possibility that the Cripto-positive cells represent a

unique side population. However, because of the disproportionately low levels of Cripto observed in these cancer cells, we suggest that it is unlikely that modulations in Cripto contributed significantly to the results obtained in our study. Furthermore, we speculate that Nodal may be propagating its signal by binding to and activating the ALK 4/7 receptor complex via a Cripto-independent mechanism (please refer to Fig. 1*D*).

In embryological systems Nodal is regulated via a positive feedback loop (1, 15). To control this system, and enable alternative cell fate decisions, endogenous inhibitors such as Lefty-A, Lefty-B, and Cerberus, are used (1, 15). In conjunction with Nodal and Oct 3/4, Lefty-A and -B are among the most enriched genes expressed in hESCs, exemplifying the putative importance of these inhibitors (17, 27). We determined that neither the cancer cells nor the normal somatic cells used in this study express Lefty. In fact Lefty expression was unique to hESCs: Other human stem cell types (including those derived from amniotic fluid, umbilical cord blood, and adult bone marrow) and embryo-associated human cytotrophoblast cells did not express appreciable levels of this protein. Furthermore, unlike H9 CMTX, matrices conditioned by these more committed stem cell lineages were unable to inhibit Nodal expression in aggressive melanoma cells. These results highlight the inherent differences between hESCs and other stem cell types, and suggest that certain therapeutic modalities may be derived exclusively from hESCs.

The results of our study demonstrate that exposure to a hESC microenvironment down-regulates Nodal signaling in melanoma and breast cancer cells, associated with a reduction in clonogenicity and tumorigenicity. However, this suppressive effect is transient and reversible. To decipher the molecular underpinnings of the suppressive effects of the hESC microenvironment on tumor cells, we focused on the deposition of Lefty (Nodal's inhibitor sequestered in the embryonic milieu) and asked whether the cancer cells that do not express Lefty could in fact respond to Lefty produced by hESCs. In a manner similar to H9 CMTX, exposure to H9-derived Lefty down-regulated Nodal expression in melanoma and breast carcinoma cells, and decreased clonogenicity in both tumor cell types as well. We were able to rescue the effect of H9-derived Lefty on clonogenicity with rNodal, suggesting that the results obtained with this treatment were due specifically to a reduction in Nodal. Further confirmation of these findings showed H9 hESCs treated with MO^{LEFTY} were unable to inhibit Nodal expression in the C8161 and MDA-MB-231 cells. In fact, exposure of these tumor cells to matrix conditioned by the Lefty-deficient hESCs resulted in a significant up-regulation of Nodal expression, which we postulate is because of a feed-forward response of Nodal-expressing tumor cells to the overproduction of Nodal by the hESCs. Finally, exposure to H9 CMTX reduced anchorage-independent growth, but in contrast to purified hESC-derived Lefty, this effect could not be completely rescued by the inclusion of rNodal. Collectively, these results suggest that Lefty plays an important role in the ability of the hESC microenvironment to suppress the tumorigenic phenotype, but that it is not the only inhibitory component.

Previous work from another laboratory reported that addition of Lefty protein to hESC cultures, even at a high, nonphysiological dose of 200 ng/ml, failed to inhibit Nodal and induce hESC differentiation (17). Our results showed that although Nodal could be inhibited in C8161 melanoma cells, it required $\geq$1,000 ng/ml of recombinant Lefty (rLefty) to reach a measurable level of response by the cells. By comparison, Lefty recovered from hESCs (plus their CMTX) inhibited Nodal in C8161 and MDA-MB-231 cells at a significantly lower concentration (estimated in the range of 20–50 ng/ml). These observations led us to examine whether rLefty is significantly different from hESC-derived Lefty in terms of glycosylation because glycosylation is typical for proteins made by eukaryote cells, but not characteristic of proteins made recombinantly (e.g., through bacterial transduction). We found that commercially available rLefty A and rLefty B are not glycosylated by using the Pro-Q Emerald 300 staining kit, whereas Lefty recovered from hESCs (plus CMTX) is glyosylated, which could ultimately affect how this protein functions physiologically, and may provide a possible explanation for these disparate observations.

Although exposure to a hESC microenvironment inhibits Nodal expression and tumorigenicity in both melanoma and breast carcinoma cells, the breast cancer cells undergo a more complex reprogramming event. Although melanoma cells respond to the hESC-derived factors within 3 days, the breast carcinoma cells require 2 additional days to achieve the most significant down-regulation in Nodal. This discrepancy is likely attributable to differences in signaling mechanisms between these two cell types. For example, although C8161 cells do not express TGF-β1, which like Nodal uses Smad-2 as a signaling mediator, MDA-MB-231 cells actively employ this system, enabling the continued phosphorylation of Smad-2, which may sustain Nodal expression for a longer duration (4, 28). Despite the inherent differences between neural crest-derived melanoma cells and epithelial-derived breast carcinoma cells, these divergent tumor types both underwent apoptosis after exposure to hESC CMTX. This remarkable similarity is likely attributable to the commonality of plasticity (e.g., the aberrant and unregulated expression of Nodal) that indiscriminately unifies highly aggressive cancer cells, regardless of their origin.

This study used an innovative approach to address whether aggressive cancer cells, expressing a plastic, embryonic-like phenotype, could respond to regulatory cues that control cell fate determination within the microenvironment of hESCs and other stem cell types. We revealed that aggressive cancer cells, but not normal cell types, express the embryonic morphogen Nodal, which is essential to the maintenance of hESC pluripotency, but unlike hESCs, the tumor cells lack Lefty, a negative regulator of Nodal. Down-regulation of Nodal expression via exposure to the hESC microenvironment (containing Lefty) resulted in a reduction in clonogenicity and tumorigenesis accompanied by an increase in apoptosis. Particularly noteworthy is the finding associated with the exclusivity of the hESC microenvironment to down-regulate Nodal expression in aggressive tumor cells, because it is not observed with other stem cell types (isolated form amniotic fluid, cord blood, or adult bone marrow) or trophoblasts, which do not express Lefty. Understanding the tumor-suppressive effect(s) of the hESC microenvironment, together with the importance of its influence on the Nodal signaling pathway, may offer new therapeutic strategies to inhibit tumor progression.

Materials and Methods

Cell Culture. Human cutaneous melanoma (C8161, WM-278) and breast carcinoma (MDA-MB-231, MCF-7, T47D, MDA-MB-468, MDA-MB-330 and ZR75–30) lines were maintained as described (29–31). Normal human neonatal epidermal melanocytes (HEMn-LP; Cascade Biologics), myoepithelial cells [Hs 578 Bst; American Type Culture Collection (ATCC)] and primary mammary epithelial cells (HMEpC; Cell Applications) were maintained as per distributor instructions. Live umbilical cord blood stem cells (SC00125; New Jersey Stem Cell Resource at Coriell Institute for Medical Research), amniotic-fluid-derived stem cells (GM00473, GM00957A) and adult bone-marrow-derived MSCs (Stem Cell Technologies) were maintained under the recommended conditions. HTR-8/SVneo is a well characterized human extravillous cytotrophoblast cell line, and was maintained as described in ref. 32. H1 and H9 hESCs (WiCell, Madison WI) and MEL-2 hESCs (Millipore) were maintained as described in ref. 14. For conditioned matrix experiments, hESCs were maintained in stem cell medium preconditioned on irradiated mouse embryonic fibroblasts (CF-1, ATCC) as described in ref. 14. Recombinant Nodal and Lefty (R&D Systems) were diluted as per manufacturer suggestions.

3D Conditioned Matrix Experiments. Conditioned matrices were prepared by using hESCs, melanocytes, myoepithelial cells, amniotic-fluid-derived stem cells, or trophoblast cells on growth factor-reduced Matrigel (14 mg/ml; BD Biosciences) as described in ref. 14. Alternatively, hESC-derived Lefty protein was seeded into Matrigel before polymerization (for complete methods outlining the

purification of Lefty, see *SI Methods*). C8161 or MDA-MB-231 cells were exposed to specific matrices preconditioned by these cells for 3 to 4 days.

Immunoblotting. Protein lysates were prepared and quantified as described in ref. 4. Equal amounts of protein were separated by SDS/polyacrylamide gel electrophoresis (PAGE) under reducing conditions, and resolved proteins were transferred onto Immobilon-P membranes (Millipore). Membranes were blocked, incubated with primary antibody (SI Table 2), washed, and incubated with the appropriate horseradish peroxidase-labeled secondary antibody. Secondary antibodies were detected by enhanced chemiluminescence (Super Signal; Pierce) with exposure to autoradiography film (Midwest Scientific).

RNA Extraction and RT-PCR. RNA was isolated by using TRIzol (Invitrogen, Carlsbad, CA) and 1 μg of was reverse transcribed as described in ref. 4. Real-time PCR was performed as described in ref. 4 by using *Taq*Man gene expression human primer/probe sets for *Lefty1/B* (Hs00764128_s1), *Nodal* (Hs00250630_s1), *Nanog* (Hs02387400_g1), and *OCT 3/4* (Hs00999632_g1). Gene expression was normalized to *18S rRNA* (Hs99999901_s1). Data were analyzed by using the Applied Biosystems Sequence Detection Software (Version 1.2.3). Semiquantitative RT-PCR was performed for *Lefty*, *Nodal*, *Cripto*, and *HPRT1* as outlined in *SI Methods*.

Immunofluorescence. Cells were fixed with 4% paraformaldehyde, made permeable with 20 mM Hepes, 0.5% Triton X-100 and blocked with serum-free protein block (DAKO). Primary antibodies were diluted in antibody dilutent (DAKO) to concentrations outlined in SI Table 2, and appropriate fluorochrome-conjugated secondary antibodies were used according to manufacturer recommendations. Nuclei were stained with DAPI (0.1 mg/ml; Invitrogen/Molecular Probes), and images were obtained by using confocal microscopy (Zeiss 510 META; Carl Zeiss).

Anchorage-Independent Growth Assays. Assays were conducted as described in ref. 4.

Glycoprotein Determination. Protein lysates underwent SDS/PAGE and transfer and were stained for glycoproteins by using the Pro-Q Emerald 300 staining kit (Molecular Probes). After drying the blot, glycoproteins were visualized by using an UV transilluminator and an image of the green fluorescing proteins were captured by using a color CCD camera (Toshiba) equipped with a deep yellow #15 filter. The blot was then rehydrated as per manufacturer's instructions and Lefty protein was detected with immunoblotting. See *SI Methods* for more in depth details.

Experimental Orthotopic Tumor Models. Five-week-old mice were injected s.c. with 250,000 C8161 cells in 50 μl of complete RPMI; or 500,000 MDA-MB-231 cells in 50 μl of complete RPMI were injected into the mammary fat pad of 6- to 8-week-old mice. When tumors became palpable measurements were taken twice per week. All experiments involving animals were approved by the Institutional Animal Care and Use Committee at the Children's Memorial Research Center.

Immunohistochemistry. Immunohistochemical staining for Nodal in a breast carcinoma progression tissue microarray (CBL-TMA-029; Creative Biolabs) was performed as described in ref. 4. In addition, tissues from the orthotopic tumor models were formalin-fixed and paraffin-embedded and immunohistochemical staining on this tissue was conducted by using a Ki67-specific antibody (SI Table 2) or ChromPure Goat IgG (Jackson Laboratories) as described in ref. 4. TUNEL assays to measure apoptosis were conducted as per manufacturer's instructions (Millipore).

Lefty Knockdown. Fluorescein (FITC)-conjugated control (5′-CCTCTTACCTCAGTTACAATTTATA-3′), Lefty-A (5′-GCCACATGGTGCTGCCCTGGG-3′) and Lefty-B (5′CTGCATGGTGCTGCCCTGGAGGA-3′) Morpholinos (20 μM) (Gene Tools) were delivered by using the scrape method (4). Cancer cells were sorted for FITC and were allowed to recover for 1 day before experimentation.

Statistical Analyses. For tumor formation studies, we determined statistical significance by using the Kruskal–Wallis one-way ANOVA on ranks, followed by Dunn's method or a one-way ANOVA followed by the Student–Newman–Keuls method for pairwise multiple comparisons. For the clonogenic assays we determined statistical significance by using ANOVA followed by the Student–Newman–Keuls method for pairwise multiple comparisons. For the correlation of breast cancer stage and Nodal expression, a Spearman rank order correlation was used. In all cases, differences were statistically significant at $P < 0.05$.

ACKNOWLEDGMENTS. We thank Drs. Zhila Khalkhali-Ellis, M. Bento Soares, Luigi Strizzi, and David Salomon for helpful scientific discussions, and Paula Pittock at the London Regional Proteomics Core at the University of Western Ontario for protein sequencing analysis. This work was supported by grants from the Illinois Regenerative Medicine Institute, U.S. National Institutes of Health (CA59702 and CA121205), and Charlotte Geyer Foundation (to M.J.C.H.), and a Canadian Institutes of Health Research Postdoctoral Fellowship (to L.-M.P.).

1. Hendrix MJ, *et al.* (2007) Reprogramming metastatic tumour cells with embryonic microenvironments. *Nat Rev Cancer* 7:246–255.
2. Hendrix MJ, Seftor EA, Hess AR, Seftor RE (2003) Vasculogenic mimicry and tumour-cell plasticity: Lessons from melanoma. *Nat Rev Cancer* 3:411–421.
3. Hoek K, *et al.* (2004) Expression profiling reveals novel pathways in the transformation of melanocytes to melanomas. *Cancer Res* 64:5270–5282.
4. Topczewska JM, *et al.* (2006) Embryonic and tumorigenic pathways converge via Nodal signaling: Role in melanoma aggressiveness. *Nat Med* 12:925–932.
5. Bittner M, *et al.* (2000) Molecular classification of cutaneous malignant melanoma by gene expression profiling. *Nature* 406:536–540.
6. Weeraratna AT, *et al.* (2002) Wnt5a signaling directly affects cell motility and invasion of metastatic melanoma. *Cancer Cell* 1:279–288.
7. Balint K *et al.* (2005) Activation of Notch1 signaling is required for beta-catenin-mediated human primary melanoma progression. *J Clin Invest* 115:3166–3176.
8. Vallier L, Alexander M, Pedersen R (2007) Conditional gene expression in human embryonic stem cells. *Stem Cells* 25:1490–1497.
9. Pierce GB, Pantazis CG, Caldwell JE, Wells RS (1982) Specificity of the control of tumor formation by the blastocyst. *Cancer Res* 42:1082–1087.
10. Kulesa PM, *et al.* (2006) Reprogramming metastatic melanoma cells to assume a neural crest-like phenotype in an embryonic microenvironment. *Proc Natl Acad Sci USA* 103:3752–3757.
11. Illmensee K, Mintz B (1976) Totipotency and normal differentiation of single teratocarcinoma cells cloned by injection into blastocysts. *Proc Natl Acad Sci USA* 73:549–553.
12. Cucina A, *et al.* (2006) Zebrafish embryo proteins induce apoptosis in human colon cancer cells (Caco2). *Apoptosis* 11:1615–1628.
13. Lee LM, Seftor EA, Bonde G, Cornell RA, Hendrix MJ (2005) The fate of human malignant melanoma cells transplanted into zebrafish embryos: Assessment of migration and cell division in the absence of tumor formation *Dev Dyn* 233:1560–1570.
14. Postovit LM, Seftor EA, Seftor RE, Hendrix MJ (2006) A 3-D model to study the epigenetic effects induced by the microenvironment of human embryonic stem cells *Stem Cells* 24:501–505.
15. Schier AF (2003) Nodal signaling in vertebrate development. *Annu Rev Cell Dev Biol* 19:589–621.
16. Yeo C, Whitman M (2001) Nodal signals to Smads through Cripto-dependent and Cripto-independent mechanisms. *Mol Cell* 7:949–957.
17. Tabibzadeh S, Hemmati-Brivanlou A (2006) Lefty at the crossroads of ''stemness'' and differentiative events. *Stem Cells* 24:1998–2006.
18. Ulloa L, *et al.* (2001) Lefty proteins exhibit unique processing and activate the MAPK pathway. *J Biol Chem* 276:21387–21396.
19. Hochedlinger K, *et al.* (2004) Reprogramming of a melanoma genome by nuclear transplantation. *Genes Dev* 16:1675–1685.
20. James D, Levine AJ, Besser D, Hemmati-Brivanlou A (2005) TGFbeta/activin/nodal signaling is necessary for the maintenance of pluripotency in human embryonic stem cells. *Development* 132:1273–1282.
21. Vallier L, Reynolds D, Pedersen RA (2004) Nodal inhibits differentiation of human embryonic stem cells along the neuroectodermal default pathway. *Dev Biol* 275:403–421.
22. Gong YP, *et al.* (2006) Overexpression of Cripto and its prognostic significance in breast cancer: A study with long-term survival. *Eur J Surg Oncol* 33:438–443.
23. Minchiotti G (2005) Nodal-dependant Cripto signaling in ES cells: From stem cells to tumor biology. *Oncogene* 24:5668–5675.
24. Bianco C, *et al.* (2006) Identification of cripto-1 as a novel serologic marker for breast and colon cancer. *Clin Cancer Res* 12:5158–5164.
25. Normanno N, *et al.* (2004) Cripto-1 overexpression leads to enhanced invasiveness and resistance to anoikis in human MCF-7 breast cancer cells. *J Cell Physiol* 198:31–39.
26. Strizzi L, *et al.* (2004) Epithelial mesenchymal transition is a characteristic of hyperplasias and tumors in mammary gland from MMTV-Cripto-1 transgenic mice. *J Cell Physiol* 201:266–276.
27. Sato N, *et al.* (2003) Molecular signature of human embryonic stem cells and its comparison with the mouse. *Dev Biol* 260:404–413.
28. Arrick BA, Korc M, Derynck R (1990) Differential regulation of expression of three transforming growth factor beta species in human breast cancer cell lines by estradiol. *Cancer Res* 50:299–303.
29. Welch DR, *et al.* (1991) Characterization of a highly invasive and spontaneously metastatic human malignant melanoma cell line. *Int J Cancer* 47:227–237.
30. Seftor EA, *et al.* (2002) Expression of multiple molecular phenotypes by aggressive melanoma tumor cells: role in vasculogenic mimicry. *Crit Rev Oncol Hematol* 44:15–27.
31. Cailleau R, Young R, Olive M, Reeves WJ, Jr (1974) Breast tumor cell lines from pleural effusions. *J Natl Cancer Inst* 53:661–674.
32. Graham CH, *et al.* (1993) Establishment and characterization of first trimester human trophoblast cells with extended lifespan. *Exp Cell Res* 206:204–211.